

# Sigma-phase in the Fe-Re alloy system: experimental and theoretical studies

J. Cieslak,\* S. M. Dubiel, J. Zukrowski, and J. Tobola  
AGH University of Science and Technology, Faculty of Physics and  
Applied Computer Science, al. Mickiewicza 30, 30-059 Krakow, Poland  
(Dated: November 9, 2018)

X-ray diffraction (XRD) and Mössbauer spectroscopy techniques combined with theoretical calculations based on the Korringa-Kohn-Rostoker (KKR) electronic structure calculation method were used to investigate  $\sigma$ -phase  $\text{Fe}_{100-x}\text{Re}_x$  alloys ( $x = 43, 45, 47, 49$  and  $53$ ). Structural data such as site occupancies and lattice constants were derived from the XRD patterns, while the average isomer shift and distribution curves of the quadrupole splitting were obtained from the Mössbauer spectra. Fe-site charge-densities and the quadrupole splittings were computed with the KKR method for each lattice site. The calculated quantities combined with the experimentally determined site occupancies were successfully used to decompose the measured Mössbauer spectra into five components corresponding to the five sublattices.

PACS numbers: 33.45.+x, 61.43.-j, 71.20.Be, 71.23.-k, 74.20.Pq, 75.50.Bb, 76.80.+y

## I. INTRODUCTION

The  $\sigma$ -FeRe is one among about fifty members of this phase known to exist in binary alloy systems, AB, where (larger) A is a transition metal element which belongs to the V-th or VI-th Group and (smaller) B-one to the VII-th or VIII-th Group of Periodic Table of Elements<sup>1,2</sup>. It is also one of five Fe-containing binary  $\sigma$ -phases. Its occurrence in the Fe-Re alloy system was definitely established in 1956<sup>3</sup>: the  $\sigma$ -phase was obtained by sintering elemental iron and rhenium powders, mixed in the proportion 3:2, at 1673 K for 4 hours. The relative concentration of the constituting elements was chosen following a phase diagram by Eggers in which a phase  $\text{Fe}_3\text{Re}_2$  was indicated<sup>4</sup>. Its characteristic features viz. hardness and brittleness were similar to those known for  $\sigma$ -phases. Especially hard was the  $\text{Fe}_3\text{Re}_2$  in the range of 45-50 at%Re. Noteworthy, neither systematic studies of  $\sigma$  in the Fe-Re alloys aimed at establishing borders of its existence nor at revealing its physical properties were carried out so far. Among known papers on the issue, one has to mention the ones reporting a successful synthesis of  $\sigma$  by an isothermal annealing of ingots of  $\text{Fe}_{55}\text{Re}_{45}$  alloys at 1763 K for 6 hours<sup>5,6</sup> as that of  $\text{Fe}_{53.6}\text{Re}_{64.4}$  at 1603 K for 8 hours<sup>7</sup>.

Here we report on a successful synthesis of seven samples of  $\sigma$ - $\text{Fe}_{100-x}\text{Re}_x$  alloys with  $x = 41, 43, 45, 47, 49, 53$  and  $55$ , nominally, and on their experimental and theoretical studies with X-ray diffraction and Mössbauer spectroscopy techniques, as well as electronic structure calculations performed with the charge and spin self-consistent Korringa-Kohn-Rostoker (KKR) Greens function method<sup>8-10</sup>.

## II. EXPERIMENTAL

The  $\sigma$ -phase was obtained in the following way: powders of elemental iron (99.9+ purity) and rhenium (99.99 purity) were mixed in appropriate proportions and masses

of  $\sim 2\text{g}$  were next pressed to pellets. The pellets were subsequently melted in an arc furnace under protective atmosphere of argon. The ingots were next remelted three times to improve their homogeneity. Finally, they were vacuum annealed at 1800 K for 5 hours and quenched into liquid nitrogen. The mass losses of the fabricated  $\sigma$ -FeRe alloys were no more than 0.01% of their initial values, so it is reasonable to take their nominal compositions as real ones. The samples were investigated with two experimental techniques viz. X-ray diffraction (XRD) and the Mössbauer spectroscopy (MS). Measurements of diffraction patterns and of Mössbauer spectra were carried out on powdered samples at room temperature (the  $\sigma$ -phase is very brittle, so it could be easily transformed into powder by attrition in an agate mortar). From the XRD patterns, an example of which is displayed in Fig. 1, we obtained an evidence that in all cases, except two border compositions, the transformation into the  $\sigma$ -phase was 100% successful. In the sample

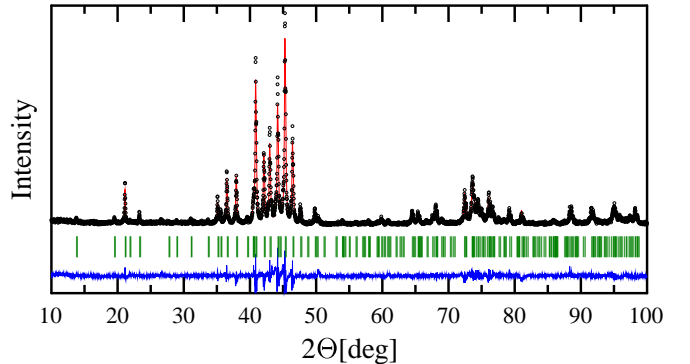


FIG. 1: (Online color) Parts of selected fitted X-ray diffractograms recorded at 294K on the  $\sigma$ -phase sample of  $\text{Fe}_{53}\text{Re}_{47}$ . The solid line stays for the best-fit obtained with the procedure described in the text. Peak positions for  $\sigma$ -phase are indicated, a difference diffractogram is shown, too.

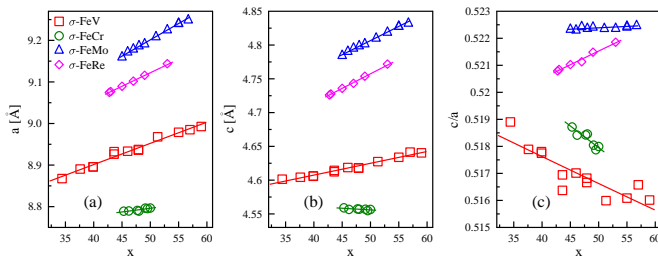


FIG. 2: (Online color) Dependence of the lattice parameters  $a$  and  $c$  as well as  $c/a$  ratio for  $\sigma\text{-Fe}_{100-x}\text{X}_x$  ( $\text{X}=\text{Cr}, \text{V}^{11}, \text{Mo}^{12}$  and  $\text{Re}$ ) versus  $x$ , as determined from the X-ray diffractograms recorded at 294K.

with the highest Re-content ( $x = 55$ ) the transformation was not fully complete, so this sample was excluded from further investigations. On the other hand, the sample with the highest Fe-content ( $x = 41$ ) was found to be fully transformed and no any traces of other phases were found. Unfortunately, the values of lattice constants as well as the volume of the unit cell did not stay in line with the corresponding results for other samples, namely they are shifted to  $x = 42.8$  so to higher Re concentrations. These values should be taken as borders of the formation of the FeRe  $\sigma$ -phase at 1800 K.

### III. RESULTS AND DISCUSSION

#### A. XRD measurements

The powder XRD patterns were collected at RT with a D5000 Siemens diffractometer (using Cu K- $\alpha$  radiation and a graphite secondary monochromator) within the  $2\theta$ -range from  $10^\circ$  to  $140^\circ$  in steps of  $0.02^\circ$ . Data were analyzed by the Rietveld method as implemented

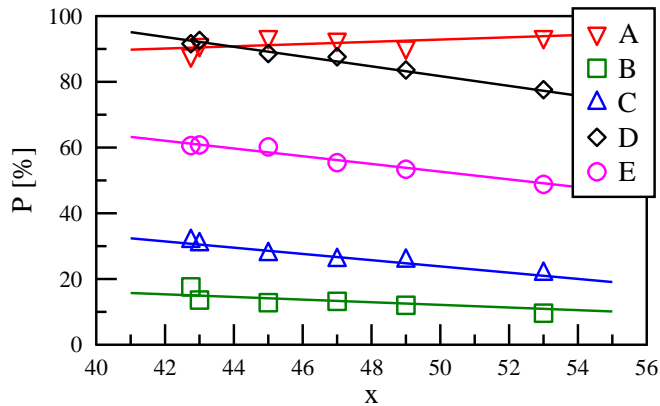


FIG. 3: (Online color) Probability of finding Fe atoms at different lattice sites in the  $\sigma\text{-Fe}_{100-x}\text{Re}_x$  compounds,  $P$ , versus Re concentration,  $x$ . Solid lines stay for the linear fits to the data

TABLE I: Atomic crystallographic positions for the five lattice sites of the Fe-Re  $\sigma$ -phase.

Site	Wyckoff index	x	y	z
A	2i	0	0	0
B	4f	0.4016(3)	0.4016(3)	0
C	8i	0.4645(2)	0.1327(4)	0
D	8i'	0.7422(5)	0.0657(3)	0
E	8j	0.1834(2)	0.1834(2)	0.2497(3)

TABLE II: Lattice constants  $a$  and  $c$  as measured for all investigated  $\sigma\text{-Fe}_{100-x}\text{Re}_x$  samples.

$x$	$a$ [Å]	$c$ [Å]
42.8	9.0749(2)	4.7261(1)
43.0	9.0767(1)	4.7276(1)
45.0	9.0895(2)	4.7359(1)
47.0	9.1019(1)	4.7433(1)
49.0	9.1159(1)	4.7538(1)
53.0	9.1438(1)	4.7717(1)

in the FULLPROF program<sup>13</sup> to get information on the crystallographic structure and the sites occupancy. From 22 free parameters used, 6 were related to a background and line positions, 10 to lattice sites occupancies and atomic positions, while the remaining 6 to line widths, lattice constants and Debye-Waller factors. The analysis yielded the lattice constants  $a$  and  $c$  (Table II, Fig. 2a,b), the atomic positions (Table I), and the lattice sites occupancies (Fig. 3).

Concerning the atomic positions, they do not depend on the samples composition within the error limit. They are also in line with those reported in the literature<sup>7</sup>. Both lattice constants show a linear dependence on the composition viz. they increase with  $x$ . Such behavior is consistent with that found for the  $\sigma$ -phase in other binary Fe-based alloys, namely Fe-Cr, Fe-V and Fe-Mo, and it is related to the atomic size of the so-called A element (here Cr, V, Mo, Re) which is larger than the size of Fe atom (1.56 Å). Also relative values of the lattice constants reflect the atomic size effect as their relative ordering follows the atomic size of Cr (1.66 Å), V(1.71 Å), Re (1.88 Å) and Mo (1.90 Å). A different trend, as illustrated in Fig. 2c, can be seen for the  $c/a$  ratio which is for the  $\sigma\text{-FeRe}$  concentration dependent increasing from 0.5207(1) to 0.5219(1). These values can be compared with 0.5211(1) given by Joubert<sup>7</sup>. For all other  $\sigma$ -phase compounds shown in this figure, the ratio either stay constant (Fe-Mo) or linearly decreases with the concentration of the element A (Cr, V).

Regarding the sites occupancies, all five sites are mixed i.e. occupied by both types of atoms - see Fig. 3 and Table III. However, sites A and D are in majority populated by Fe atoms, while sites B and C are mostly occupied by Re atoms. The population of Fe/Re atoms on site E is rather in balance, yet the probability of finding an Fe

TABLE III: Fe-occupancies, isomer shift,  $IS$  and quadrupole splitting,  $QS$  for the  $\sigma$ -Fe<sub>53</sub>X<sub>47</sub> (X=Cr<sup>11,14</sup>, V<sup>11,15</sup>, Mo<sup>12</sup> and Re)

Site	Fe-occupancy [%]				IS [mm/s]				QS [mm/s]			
	V	Cr	Mo	Re	V	Cr	Mo	Re	V	Cr	Mo	Re
A	93.2	87.8	100.0	91.8	-	-	-	-	0.351	0.342	0.280	0.598
B	18.2	27.2	12.9	13.3	0.341	0.351	0.303	0.260	0.292	0.242	0.404	0.616
C	35.2	40.5	25.5	26.7	0.201	0.216	0.205	0.246	0.282	0.181	0.329	0.587
D	96.3	89.2	100.0	86.2	0.012	0.023	0.023	0.067	0.209	0.210	0.208	0.352
E	34.9	33.5	41.9	56.2	0.115	0.113	0.113	0.141	0.454	0.454	0.464	0.640

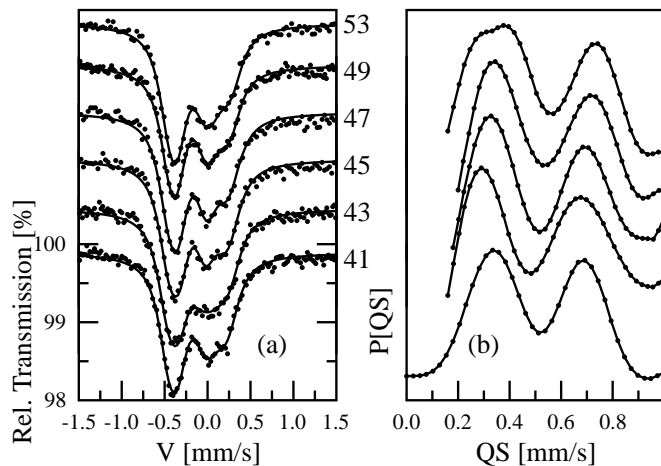


FIG. 4: (a)  $^{57}\text{Fe}$  Mössbauer spectra recorded on a series of  $\sigma$ -Fe<sub>100-x</sub>Re<sub>x</sub> samples at 294K and marked with the corresponding  $x$ -values. The solid lines are the best-fit to the experimental data. The derived quadrupole splitting distribution curves shown in the same sequence as the spectra, are indicated in (b).

atom on this site linearly decreases with  $x$  from  $\sim 60\%$  for  $x = 43$  to  $\sim 50\%$  for  $x = 53$ . A similar trend is observed for the sites B, C and D. An exceptional trend exhibits the site A for which the occupancy in Fe atoms slightly increase with  $x$ .

It is interesting to compare the sites occupancies in different Fe-X alloy systems. A range of composition where the  $\sigma$ -phase can be formed is characteristic of the system. However, the range of  $x = 45 - 50$  is common, so a comparison of the sites occupancies for a concentration from that range seems reasonable. Appropriate data for  $x = 47$  are displayed in Table III. It is evident that the sites A and D are predominantly (exclusively, for Fe-Mo) occupied by Fe atoms irrespective of the alloy system. The lowest population of Fe atoms is typical of the site B (27%, at maximum). The occupancies of the sites C and E behave in a way characteristic of the A element: for Cr the site C is more populated by Fe atoms than the site E, while for Mo and Re the opposite is true. Finally, for V the C and E sites host about the same number of Fe atoms.

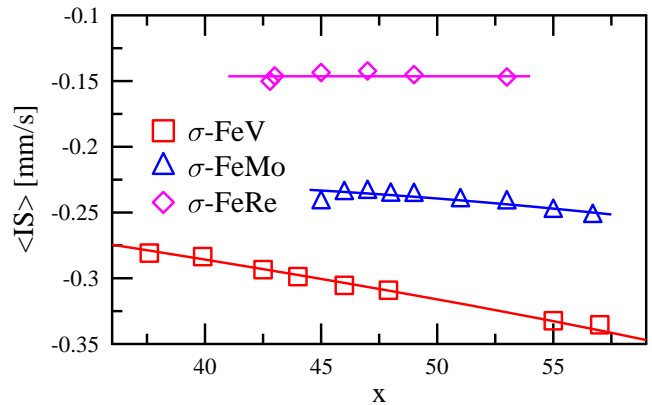


FIG. 5: (Online color) The average isomer shift (relative to the Co/Rh source),  $\langle IS \rangle$ , versus concentration,  $x$ , as measured (markers) and as calculated (lines) for  $\sigma$ -Fe<sub>100-x</sub>X<sub>x</sub> (X=Cr<sup>14</sup>, V<sup>15</sup>, Mo<sup>12</sup> and Re).

## B. Mössbauer measurements

$^{57}\text{Fe}$  spectra which were recorded at 295 K in a transmission mode using a standard spectrometer and a  $^{57}\text{Co}/\text{Rh}$  source for the gamma rays are presented in Fig. 4. They are very asymmetric, which was not observed for other  $\sigma$ -phase Fe-X (X=Cr, V, Mo) alloys. But as in the previous cases, the structure of the spectra is badly resolved which did not allow to analyze them in terms of a superposition of subspectra corresponding to the five sublattices. Instead, they were fitted assuming a distribution of the quadrupole splitting,  $QS$ , and a linear correlation between  $QS$  and the isomer shift,  $IS$ <sup>16</sup>. The analysis yielded the distribution curves of  $QS$ , that are

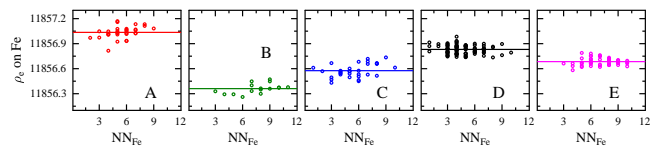


FIG. 6: (Online color) Fe-site charge density,  $\rho_e$ , for five crystallographic sites versus  $NN_{\text{Fe}}$ . Solid lines represent average values of  $\rho_e$

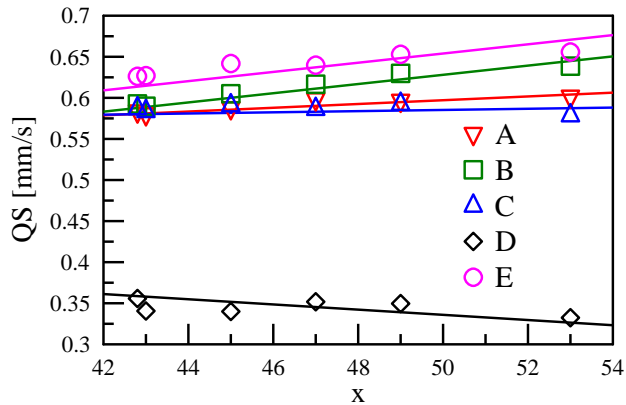


FIG. 7: (Online color) Quadrupole splitting,  $QS$ , as determined for each site and Re concentration,  $x$ , from the analysis of the measured spectra with the protocol described in Ref. 14.

displayed in Fig. 4b, as well as the average isomer shifts,  $\langle IS \rangle$  - see Fig. 5. Concerning the  $QS$ -values, it is evident that their distribution has two maxima: one at about 0.35 mm/s, the other at about 0.75 mm/s. The average isomer shift does not practically depend on the composition which means the average Fe-site charge density is the same in all investigated samples. This is different in comparison with the  $\sigma$ -phase in Fe-Mo and Fe-V alloys, where, as indicated in Fig. 5, one observes a weak linear decrease of  $\langle IS \rangle$  with the concentration of Mo and V, respectively<sup>12,15</sup>.

### C. Electronic structure calculations

The electronic structure of the  $\sigma$ -phase can be calculated at the level of particular lattice sites as already shown for the  $\sigma$ -phase in Fe-X (X=Cr, V, Mo) alloys<sup>12,14,15</sup>. In particular, one can calculate  $QS$  and  $IS$ -values for each site, and next use them to successfully fit the Mössbauer spectra. In the present case, the calculations were carried out for 16 unit cells having different configurations of Fe/Re atoms over the five sublattices. The configurations were chosen following two criteria: (1) the probability of finding Fe/Re atoms on a given sublattice should be as close as possible to the one determined experimentally, and (2) each possible configuration of atoms with a given number of Fe atoms occupying the nearest-neighbour position,  $NN$ , should be represented at least once. Charge-densities obtained with this protocol,  $\rho_{Fe}$ , were expressed in terms of the number of Fe atoms situated in  $NN$ ,  $NN_{Fe}$ , for each of the five sublattices. Using next a linear relationship between  $IS$  and  $\rho_e$ <sup>17</sup>, the calculated  $\rho_e$ -values for each sublattice were re-calculated into  $IS$ -values, and finally into the average one for each spectrum,  $\langle IS \rangle$ . The calculated potentials in combination with the experimentally determined site

occupancies were used to determine the  $QS$ -values for each sublattice and composition. The calculations were done using the extended point-charge model as outlined elsewhere<sup>14,15</sup>. The charge-densities obtained with the above mentioned protocol and method are visualized in Fig. 6 for each sublattice. As in the case of  $\sigma$ -FeMo<sup>12</sup>, the  $\rho_e$ -values are rather  $NN_{Fe}$  independent which was not the case for  $\sigma$  in Fe-Cr and Fe-V alloys<sup>14,15</sup>. Consequently, the average values of the charge-densities, hence those of the isomer shifts for the given lattice sites were calculated as an average over all atomic configurations taken into account in the calculations for that sites. The  $\langle IS \rangle$ -values were calculated as the average over all five sites and were in a good agreement with those found from the Mössbauer spectra fitting (Fig. 5). The data shown in Fig. 6 give a possibility for making a comparison between the charge-densities on particular lattice sites. It is evident that the highest charge-density have Fe atoms on sites A, followed by those on D, E, C and B. One can also make a comparison between the calculated site densities for the five sublattices in different alloy systems we studied so far. The appropriate data, expressed in terms of the isomer shifts, are displayed in Table III. The  $IS$ -values of particular sites are given relative to that of the site A which was found to have the highest charge-density. It is evident that for all studied alloys that the smallest  $IS$ -value, hence the highest charge-density among the remaining four sites, have Fe atoms on the site D followed by the sites E, C and B.

The calculated values of the quadrupole splitting,  $QS$ , are shown in Fig. 7. It is clear that the lowest field gradient was found on the site D,  $QS = 0.3$ - $0.35$  mm/s, while those on the other four sites are much larger (almost by a factor of 2) and close to each other. The difference between them slightly increases with  $x$ . Based on these calculations one can understand the two-peak structure of the experimentally obtained  $QS$ -distribution curves (Fig. 4b). A set the  $QS$ -values calculated for the different lattice sites and alloys for  $x = 0.47$  is presented in Table III. It is clear that the  $QS$ -values found for the Fe-Re samples are meaningfully higher than the corresponding quantities calculated for the other studied Fe-X alloys. This observation seems to agree with the fact that Re atoms have a large atomic size (only Mo atoms are larger here, but the unit cell of the FeRe  $\sigma$ -phase is smaller), hence they cause the asymmetric-most distribution of the charge around the probe Fe atoms. Noteworthy, the smallest  $QS$ -values were calculated for the site D, and the largest ones for the site E.

### D. Mössbauer spectra analysis

The knowledge of the lattice site occupancies combined with that of the calculated  $IS$  and  $QS$  values permitted to carry out the analysis of the Mössbauer spectra in terms of the five sublattices. A successful analysis could have been done with only five free parameters. Four of

them viz. background, spectral area, line width (common for all five subspectra) and the isomer shift of one subspectrum depend on the conditions of the spectra measurements, hence they could not be calculated. The fifth free parameter was a proportionality constant between the calculated maximum component of the electric field gradient,  $V_{zz}$ , in which only the so-called lattice contribution was taken into account, and  $QS$ , in which also a contribution from electrons localized on the probe atom is included. Two examples of the measured spectra analyzed in this way are presented in Fig. 8 together with the subspectra belonging to the five sublattices. A very good agreement between the measured and fitted spectra was achieved.

#### IV. SUMMARY AND CONCLUSIONS

Six samples of the  $\sigma$ -phase  $\text{Fe}_{100-x}\text{Re}_x$  alloys ( $x = 43, 45, 47, 49, 53$  and  $55$ ) were synthesized and experimentally investigated using X-ray diffraction and Mössbauer spectroscopy techniques, and theoretically with the electronic structure calculations using Korringa-Kohn-Rostoker method. XRD yielded information on

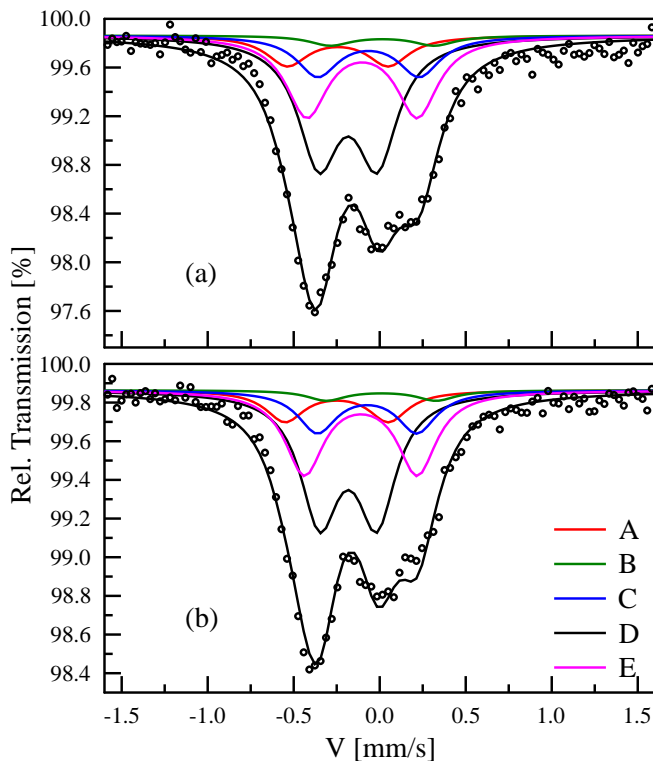


FIG. 8: (Online color)  $^{57}\text{Fe}$ -site Mössbauer spectra recorded at 294K on two studied samples viz. with (a)  $x = 45$  and (b)  $x = 53$ . The best-fit spectrum and five subspectra are indicated by solid lines.

site occupancies and lattice constants, MS on the average isomer shift and a distribution of the quadrupole splitting. Charge-densities and the quadrupole splittings were computed with the KKR method. The calculated quantities combined with the experimentally determined site occupancies were successfully used to analyze the measured Mössbauer spectra.

Based on the results reported in this paper, the following conclusions can be made:

- A pure  $\sigma$ -phase in the  $\text{Fe}_{100-x}\text{Re}_x$  alloy system at 1800K can be formed for  $x$  between 43 and 53.
- Its lattice parameters  $a$  and  $c$  show a linear increase with  $x$ , the  $c/a$  ratio also increases.
- The site occupancies are mixed i.e. both Fe and Re atoms can be found on all five sites. However, the sites A and D are predominantly occupied by Fe atoms, while Re atoms are in majority on the sites C and B. The population of both types of atoms on the site E is in a fair balance.
- The calculated Fe-site charge-density,  $\rho_e$ , are characteristic of the lattice site, they are rather independent of the number of Fe atoms in the first-neighbor shell, and they increase in the following order:  $\rho_e(A) > \rho_e(D) > \rho_e(E) > \rho_e(C) > \rho_e(B)$ .
- The average isomer shift,  $\langle IS \rangle$ , derived from the analysis of the measured spectra is independent of the alloys composition. This behavior can be explained by the calculated charge-densities.
- The calculated quadrupole splitting has the lowest value for the site D, while its values for the other sites are close to each other and are by a factor of about two higher. The calculations are in line with the two-peak structure of the  $QS$ -distribution curves derived from the measured spectra.
- The calculated hyperfine quantities permitted to successfully decompose the measured spectra into five components corresponding to particular lattice sites.

#### Acknowledgments

This work was supported by the Ministry of Science and Higher Education, Warsaw (grant No. N N202 228837).

---

\* Corresponding author: cieslak@fis.agh.edu.pl

- <sup>1</sup> E. D. Hall and S. H. Algie, *Metall. Rev.* **11**, 61 (1966).
- <sup>2</sup> A. K. Sinha, *Prog. Mater. Sci.* **15**, 79 (1972).
- <sup>3</sup> J. Niemiec and W. Trzebiatowski, *Bull. Acad. Pol. Sci.* **4**, 601 (1956)
- <sup>4</sup> H. Eggers, *Mitt. Kaiser-Wilhelm-Inst., Eisenforsch.* **20**, 147 (1938)
- <sup>5</sup> C.V. Kopetskii, V.S. Shekhtman, N.V. Ageev and E.M. Savitskij, *Dokl. Akad. Nauk SSSR* **125**, 87 (1959)
- <sup>6</sup> N.V. Ageev and *Dokl. Akad. Nauk SSSR* **135**, 309 (1960)
- <sup>7</sup> J.-M. Joubert *Prog. Mater. Sci.* **53**, 528 (2008).
- <sup>8</sup> ed. by, W. H. Butler, P. Dederichs, A. Gonis, and R. Weaver, *Chapter III, in: Applications of Multiple Scattering Theory to Materials Science*, vol. 253 (MRS Symposia Proceedings, MRS Pittsburgh., 1992).
- <sup>9</sup> T. Stopa, S. Kaprzyk, and J. Tobola, *J. Phys.: Condens. Matter* **16**, 4921 (2004).
- <sup>10</sup> A. Bansil, S. Kaprzyk, P. E. Mijnders, and J. Tobola, *Phys. Rev. B* **60**, 13396 (1999).
- <sup>11</sup> J. Cieslak, M. Reissner, S. M. Dubiel, J. Wernisch and W. Steiner, *J. Alloys Comp.* **460**, 20 (2008).
- <sup>12</sup> J. Cieslak, S. M. Dubiel, J. Przewoznik and J. Tobola, To be published , (2012).
- <sup>13</sup> J. Rodriguez-Carjaval, *Physica B* **192**, 55 (1993).
- <sup>14</sup> J. Cieslak, J. Tobola, S. M. Dubiel, S. Kaprzyk, W. Steiner and M. Reissner, *J. Phys.: Condens. Matter.* **20**, 235234 (2008).
- <sup>15</sup> J. Cieslak, J. Tobola, and S. M. Dubiel, *Phys. Rev. B* **81**, 174203 (2010).
- <sup>16</sup> G. Le Caer, and R. A. Brandt, *J. Phys. Condens. Matter*, **10** 10715 (1998).
- <sup>17</sup> F. Neese, *Inorganica Chimica Acta* **337**, 181 (2002).